

Experimental evidences of a structural and dynamical transition in fish school

Ch. Becco^{a,*}, N. Vandewalle^a, J. Delcourt^b, P. Poncin^b

^aGRASP, Department of Physics B5a, Sart-Tilman, University of Liège, B-4000 Liège, Belgium

^bBiology Behaviour Unit: Ethology and Animal Psychology, Zoological Institute, University of Liège, Quai van Beneden 22, B-4020 Liège, Belgium

Received 3 October 2005; received in revised form 17 November 2005

Available online 5 January 2006

Abstract

We have developed a video tracking system in order to determine all the trajectories of young fish (*Oreochromis niloticus* L.) within a school. Both individual and collective behaviours have been studied as a function of the number of fish per unit area. By studying distributions of distances between fish and distributions of relative orientations, structural effects and cooperative motions have been evidenced. Signatures of a phase transition have been found, as predicted by some numerical models. This work opens new perspectives in the study of collective phenomena in biological systems since it is the first time that such measurements are possible.

© 2006 Elsevier B.V. All rights reserved.

Keywords: Multi-tracking; School-behaviour; Phase transition

Numerous fish species are observed to form schools [1,2]. Previous studies addressed the problem of those structures, in which making movement decisions often depend on the social interaction among group members [3]. However, several relevant questions remain open. How individual behaviours lead to a complex collective motion [4–6]? What are the characteristics of the social interaction between individuals? According to Partridge [2], every fish fits its swimming activity to the speed and direction of its neighbours. These behaviours leading to collective effects may to some extent be governed by various factors such as vision, fluid motion, fish number, etc.

Fish schools possess many similarities with physical systems. Indeed, a school may be considered as a large number of interacting entities. In this respect, some models [3,7–10] of self-propelled particles (SPP) have been recently proposed. The underlying mechanism concerns identical particles following the mean velocity of their nearest neighbours. With the help of such SPP models, complex collective features have been obtained. Particularly, a phase transition between polarized and randomly oriented SPP has been predicted as a function of the particle density [8,11].

*Corresponding author.

E-mail address: c.becco@ulg.ac.be (Ch. Becco).

A question of importance is the existence of such a phase transition in the real world. In order to corroborate physical/biological models with real fish schools, quantitative observations and precise measurements are needed. This point is the main motivation of the present work. We have experimentally studied the behaviour of young fish in a school by tracking the motion of every fish in the system. Physical characteristics, such as the correlations, have been measured as a function of the fish density. The experimental approach we propose is original and allows a precise statistical study by means of large amounts of data.

Our experimental setup is the following. A thin container ($40\text{ cm} \times 30\text{ cm} \times 2\text{ cm}$) is filled with water. Nile Tilapias (*Oreochromis niloticus* L.) fish are placed inside this flat aquarium. This particular geometry is convenient in order to track fish with a single video recorder. Young tilapia fish (see Fig. 1a) have been chosen for this study because their activity is high enough to perform measurements on a few minutes. The fish are thus constrained to move in a nearly two-dimensional space. Specimens were between 3 and 5 weeks old with a size ranging between 11 and 15 mm. This species is known to adopt schooling and shoaling behaviours at this age. The unique parameter which has been varied in our study is the surface density ρ of fish (expressed in fish per m^2). A homogeneous light source is placed above the container and a CCD camera records the fish from below. In order to avoid fish sticking along the borders of the container, we have focused our analysis into the $33\text{ cm} \times 25\text{ cm}$ central part of the container. After some image treatment, the fish appear in dark on the pictures. Our algorithm is then used to extract trajectories from these images. Its main task is to correctly associate some dark spot from one picture at time t with another dark spot on the picture taken at time $t + \Delta t$, and so for each fish. It is mainly based on spatial correlations and the knowledge of the former trajectories. Our algorithm considers also the possibility for two fishes to meet and then separate after a crossing of their trajectories. On the images, such an event results in the melting of two fish spots into a single dark spot, which later splits into two spots. Moreover, the tracking algorithm takes into account entering and leaving fish in the camera field of view. So, by correlating successive pairs of images, fish trajectories are determined allowing measurements of fish positions and velocities. Fig. 1 presents typical trajectories of all fish over a long period and for two typical cases. The acquisition time varied typically between 20 and 50 s, corresponding to a number of images ranging between 500 and 1250. Those characteristic times are large enough to get the whole

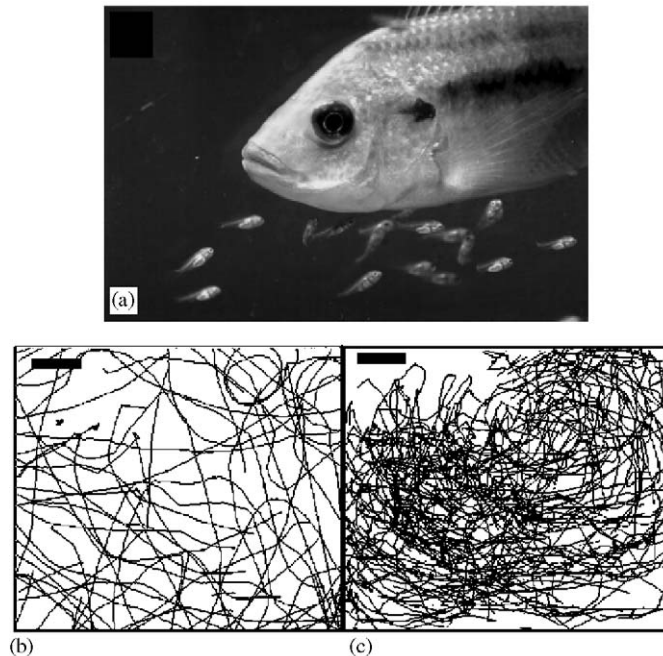


Fig. 1. (a) A picture of a female Tilapia and her “babies”. (b) The complete trajectories of 20 fish tracked during 41 s for a fish density $\rho = 350\text{ f/m}^2$. (c) The same illustration but with a fish density $\rho = 905\text{ f/m}^2$. For each picture, a $5\text{ cm} \times 1\text{ cm}$ scale is included.

system visited by the fish since trajectories cover the entire zone and the value of the typical mean speed is equal to 4 ± 1 cm/s. This is clearly revealed in Fig. 1. The maximum number of fish which can be tracked on the pictures is about 80. The maximum number is mainly determined by the resolution of the pictures.

From fish positions and fish velocities, the structure of the school can be studied. For every fish on every picture, we compute the shortest distance D to another fish in the system (see Fig. 2). Fig. 3 presents distributions of these nearest neighbour distances cumulated over all images. Two different fish densities are

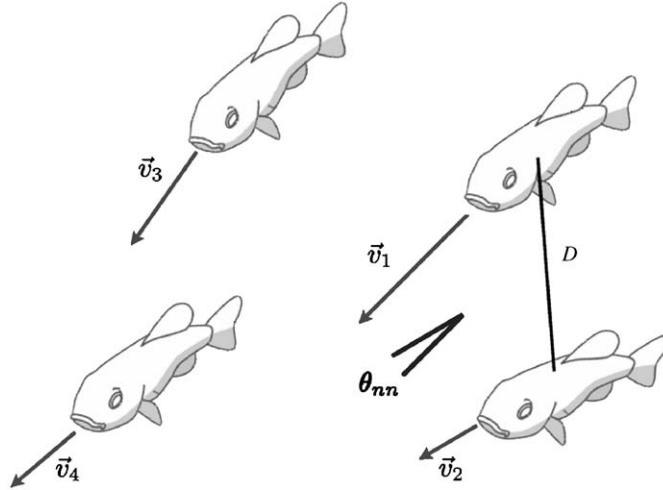


Fig. 2. Each fish is labelled and has a position and a velocity. For each fish, the shortest distance D between neighbouring fish is determined. The angle θ_{nn} as the difference of orientations between the velocities of nearest neighbouring pairs is also determined.

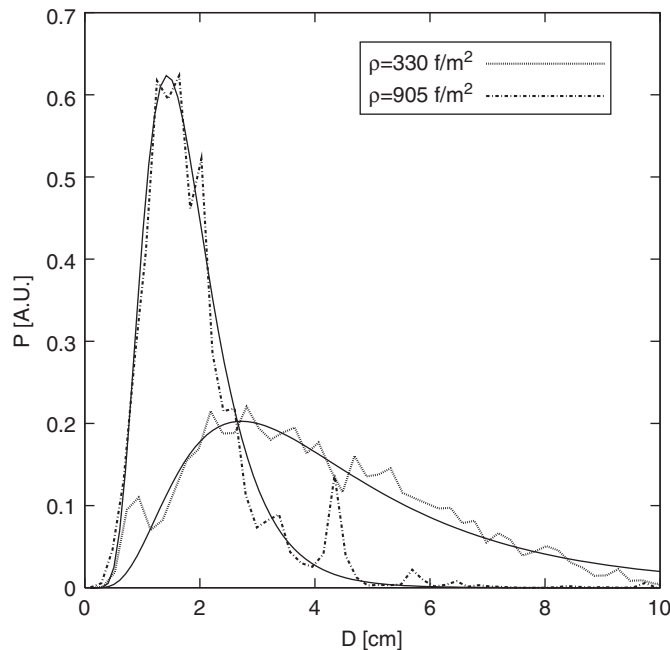


Fig. 3. Typical normalized distributions of nearest neighbour distances. Two different fish densities are illustrated. Each distribution is obtained by accumulating the positions from all the fish in all images of each movie. Distributions are well fitted with lognormal laws, given by Eq. (1). Each distribution exhibits a maximum noted D_1 . The peak observed at $D = 4$ cm represents less than 3.5% of all the data and therefore is poorly relevant.

illustrated. The distances are found to be distributed following a lognormal law, i.e.,

$$P(D) = \frac{1}{DS\sqrt{2\pi}} \exp\left(-\frac{(\log(D) - \mu)^2}{2S^2}\right), \quad (1)$$

where μ is a scale parameter and S is the shape parameter. We then compute the parameter D_1 as the position of the maximum in the distribution, i.e., $D_1 = \exp(\mu - S^2)$. The evolution of this most probable distance D_1 as a function of the density ρ is presented in Fig. 4. Even for low density values, the distance D_1 is half the distance that one expects for a homogeneous dispersion of fish in the aquarium. Therefore, fish can be viewed as attracting entities with a characteristic interdistance being a function of the density. The interdistance D_1 decreases rapidly as ρ increases, meaning that the group of fish becomes more compact at high fish densities. When the density becomes larger than 500 fish/m², the distance between fish is fixed to a minimum characteristic length close to the mean fish size. In order to emphasize different dynamical regimes for low and high densities, we have fitted the behaviour of $D_1(\rho)$ with a purely empirical law

$$D_1 = \begin{cases} a_1 (\rho_c - \rho)^\alpha + D_{1,\infty} & \text{when } \rho < \rho_c, \\ D_{1,\infty} & \text{when } \rho \geq \rho_c, \end{cases} \quad (2)$$

where a_1 is a free fitting parameter. This law defines a critical density $\rho_c = 527 \text{ f/m}^2$ and the high density limit of D_1 is about $D_{1,\infty} = 1.21 \pm 0.17 \text{ cm}$, which is approximatively 90% of the mean fish length. We have obtained $\alpha = 0.7 \pm 0.3$ for the exponent. This abrupt collapse of the interdistances in the school is a clear signature of a structural change occurring at $\rho_c = 527 \pm 126 \text{ f/m}^2$. This effect is not solely geometrical. To underline this fact, we have plotted in Fig. 4 the curve of the interdistance $D = 1/\sqrt{\rho}$ of fish spread off in all the container. It shows clearly that the fish do not occupy all the available space, so the mean interdistance is not directly dependent of the total space. Moreover, our results on the interdistances are in quite good agreement with the ones obtained in the numerical model of Ref. [9]. Their plot of the nearest neighbor distance as a function of the number of agents displays a drop with the increasing size of the group, in a

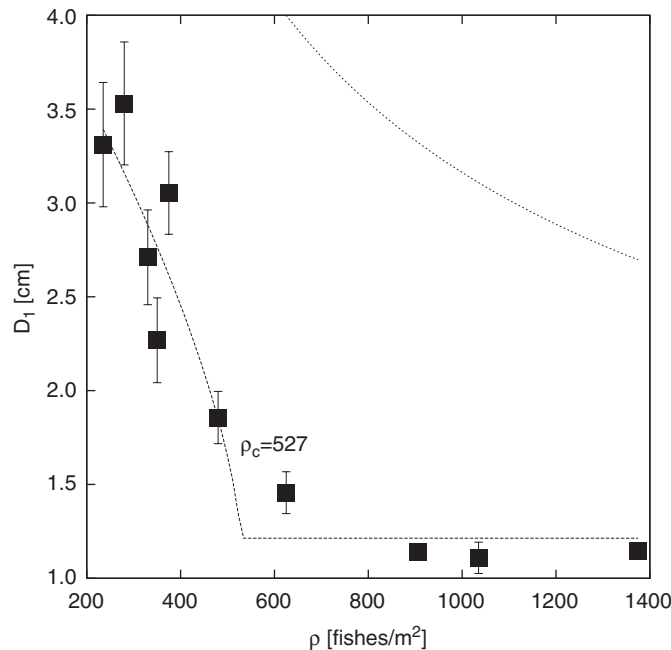


Fig. 4. The most probable interdistance D_1 in all pairs of neighbouring fish as a function of the fish density. A fit using Eq. (2) emphasizes a structural change of the school occurring for $\rho_c = 527 \pm 126 \text{ f/m}^2$. The expected distance $D = 1/\sqrt{\rho}$ for a homogeneous dispersion of fish is displayed, in the upper right corner of the plot.

manner quite similar to ours. In both cases, our experiment and the model of Ref. [9], the presence of a well-defined minimum distance for high group size has not been evidenced. The distance is varying with the number of fish.

In order to study the school dynamics, we have also measured correlations between different fish velocities. We have only considered orientations. In fact, the correlation between speeds of neighbouring fish has been found to be surprisingly very weak. However, the correlations over the relative orientations of neighbouring fish are strong. Fig. 5 presents the distribution $P(\theta_{nn})$ of the angles θ_{nn} defined (see Fig. 2) between the velocities for all pairs of nearest neighbouring fish. This distribution is peaked around zero, meaning that nearest neighbouring fish tend to swim as their kin. To compute easily the width of the distribution, an exponential fit is performed:

$$P(\theta_{nn}) = -a_2 \exp\left(-\frac{|\theta_{nn}|}{\sigma}\right) + b_1, \quad (3)$$

where a_2 and b_1 are free fitting parameters. The inverse of the width σ^{-1} measures the cooperativeness of the school. Indeed, a sharp peak in $P(\theta_{nn})$ corresponds to a strongly polarized fish group. The parameter is also plotted as a function of the fish density in Fig. 6. The results are fitted by an empirical law similar to Eq. (2). One has

$$\sigma^{-1}(\rho) = \begin{cases} b_2 & \text{when } \rho < \rho_c, \\ a_3(\rho - \rho_c)^\beta + b_2 & \text{when } \rho \geq \rho_c, \end{cases} \quad (4)$$

where a_3 and b_2 are free fitting parameters. A sharp change in cooperativeness is indeed observed around 472 f/m^2 . We have obtained $\beta = 0.7 \pm 0.3$ for the exponent.

Our results show clearly that structural and dynamical changes occur as a function of the fish density. This kind of transition, detected roughly at 500 fish/m^2 , separates two kinds of behaviours: an extended school of unpolarized fish and a compact school of polarized fish. At low densities, the environment pressure (the limitation of the space) is not so high and the fish align themselves loosely. At higher density values, as fish are

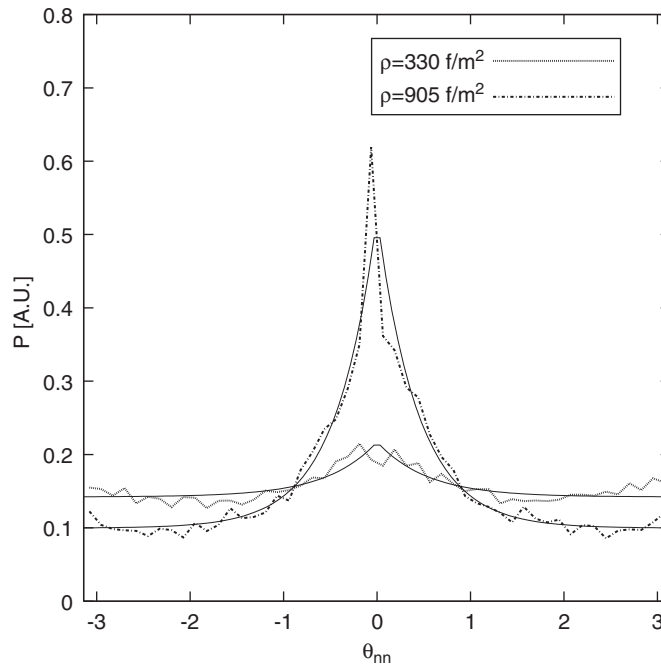


Fig. 5. Typical distributions for the relative orientations θ_{nn} in all pairs of nearest neighbouring fish. The maximum of the distribution for $\theta_{nn} = 0$ indicates that a large number of nearest neighbouring fish swim in the same direction. This number is larger when the fish density becomes high. An exponential fit using Eq. (3) is displayed.

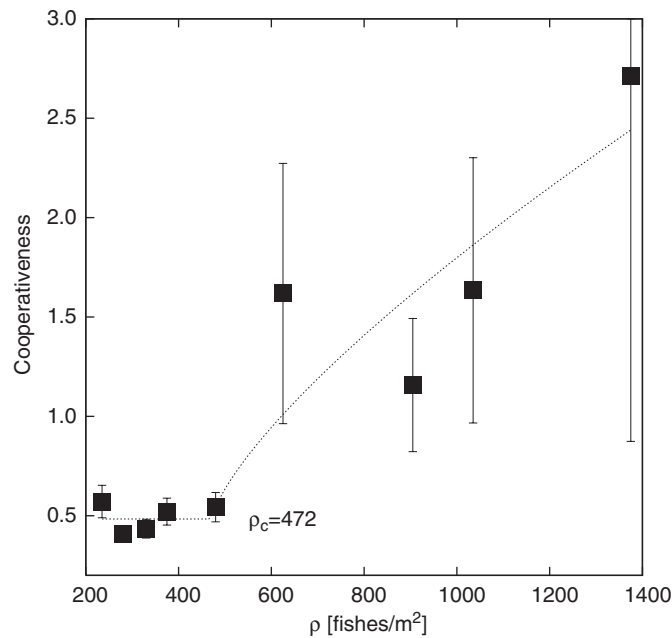


Fig. 6. The inverse of the width σ of the $P(\theta_{nm})$ distribution as a function of the fish density. This plot captures the cooperativeness σ^{-1} of the fish. A high value of σ^{-1} indicates a strong fish polarization. A fit using Eq. (4) is displayed and the critical value is found to be $\rho_c = 472 \pm 38 \text{ f/m}^2$.

more constrained, the orientation on the neighbourhood becomes stronger. The value of ρ_c is supported by two experimental evidences, from the distances and the orientations. The exact value of ρ_c is restricted to the young Tilapia fish we studied here. This experimental result is, however, quite similar to what was predicted by physical models [4,8]. Indeed, these models exhibit a transition in the polarization (σ^{-1}) of the SPP as a function of the particle density and even they do not consider variable speeds. From both key parameters considered in SPP models (density and noise), the first one is here confirmed to play an important role in the school formation.

In summary, comparison between observations and theoretical models is prevalent in the recent studies of shoals [12,13]. Our statistical study, conducted in large group of fish, demonstrates that they behave like attracting entities in a school. Moreover, they select the mean orientation of their neighbours. The main parameters in school formation are thus fish positions and relative orientations. A sharp phenomenon like a phase transition has been evidenced: proximity leads to more polarized fish as predicted by earlier physical models.

One should also note that the new automatized method we developed opens perspectives in the study of large living systems.

This research was conducted with the financial support of the FNRS (projects FRFC number 2.4544.02 and FRFC number 2.4469.06) and the support of the contract ARC 02/07-293.

References

- [1] E. Shaw, Schooling fishes, *Am. Sci.* 66 (1978) 166.
- [2] B.L. Partridge, The structure and function of fish schools, *Sci. Am.* 246 (1982) 90.
- [3] I. Couzin, J. Krause, N. Franks, S. Levin, Effective leadership and decision-making in animal groups on the move, *Nature* 433 (2005) 513.
- [4] T. Vicsek, A question of scale, *Nature* 411 (2001) 421.
- [5] T.J. Pitcher, J.K. Parrish, *Behaviour of Teleost Fishes*, second ed., Chapman & Hall, London, 1982.

- [6] J. Toner, Y. Tu, Flocks, herds, and schools: a quantitative theory of flocking, *Phys. Rev. E* 58 (4) (1998) 4828.
- [7] J. Parrish, S. Viscido, D. Grünbaum, Self-organized fish schools: an examination of emergent properties, *Biol. Bull.* 202 (2002) 296.
- [8] A. Czirók, T. Vicsek, Collective behavior of interacting self-propelled particles, *Physica A* 281 (2000) 17.
- [9] H. Kunz, C.K. Hemelrijk, Artificial fish schools: collective effects of school size, body size, and body form, *Artif. Life* 9 (3) (2003) 237–253.
- [10] G. Grégoire, H. Chaté, Onset of collective and cohesive motion, *Phys. Rev. Lett.* 92 (2) (2004) 025702.
- [11] T. Vicsek, A. Czirók, E. Ben-Jacob, I. Cohen, O. Shochet, Novel type of phase transition in a system of self-driven particles, *Phys. Rev. Lett.* 75 (6) (1995) 1226.
- [12] D. Hoare, I. Couzin, J.-G.J. Godin, J. Krause, Context-dependent group size choice in fish, *Anim. Behav.* 67 (2004) 155.
- [13] S. Viscido, J. Parrish, D. Grünbaum, Individual behavior and emergent properties of fish schools: a comparison of observation and theory, *Mar. Ecol. Prog. Ser.* 273 (2004) 239.